JOURNAL OF SPACECRAFT AND ROCKETS
Vol. 48, No. 4, July–August 2011

Matrix Methods for Optimal Manifesting of Multinode Space Exploration Systems

Paul T. Grogan,* Afreen Siddiqi,† and Olivier L. de Weck‡
Massachusetts Institute of Technology, Cambridge, Massachusetts 02139

DOI: 10.2514/1.51870

This paper presents matrix-based methods for determining optimal cargo manifests for space exploration. An exploration system is defined as a sequence of in-space and on-surface transports between multiple nodes coupled with demands for resources. The goal is to maximize value and robustness of exploration while satisfying logistical demands and physical constraints at all times. To reduce problem complexity, demands are abstracted to a single class of resources, and one metric (e.g., mass or volume) governs capacity limits. Matrices represent cargo carried by transports, cargo used to satisfy demands, and cargo transferred to other transports. A system of equations enforces flow conservation, demand satisfaction, and capacity constraints. Exploration system feasibility is evaluated by determining if a solution exists to a linear program or network-flow problem. Manifests are optimized subject to an objective function using linear or nonlinear programming techniques. In addition to modeling the manifesting problem, a few metrics such as the transport criticality index are formulated to enable analysis and interpretation. The proposed matrix manifest modeling methods are demonstrated with a notional lunar exploration system composed of 32 transports, including eight cargo and nine crewed landings at an outpost at the lunar south pole and several surface excursions to Malapert Crater and Schrödinger Basin. It is found that carry-along and prepositioning logistics strategies yield different manifesting solutions in which transport criticality varies. For the lunar scenario, transport criticality is larger for a prepositioning strategy (mean value of 3.02), as compared with an alternative carry-along case (mean value of 1.99).

Nomenclature

$\mathbf{C}$	=	transport cargo capacity vector
c_i	=	cargo capacity of transport i
$\mathbf{D_e}$	=	exploration demand vector
$\mathbf{D_t}$	=	transport demand vector
$d_{e,i}$	=	cargo demand during exploration i
$d_{t,i}$	=	cargo demand during transport i
$\mathbf{N_d}$	=	destination node vector
$\mathbf{N_o}$	=	origin node vector
n	=	number of transports
$n_{d,i}$	=	destination node of transport i
$n_{o,i}$	=	origin node of transport i
$\mathbf{S}$	=	set of source nodes
$\mathbf{T}$	=	cargo transfer matrix
$\mathbf{T_a}$	=	arrival-time vector
$\mathbf{T_d}$	=	departure-time vector
$t_{a,i}$	=	arrival time of transport i
$t_{d,i}$	=	departure time of transport i
$t_{\max}$	=	maximum dormant cargo time
$\mathbf{U_e}$	=	exploration cargo utilization matrix
$\mathbf{U_t}$	=	transport cargo utilization matrix
$u_{e,ij}$	=	cargo manifested on transport i used to satisfy demands during exploration j
$u_{t,ij}$	=	cargo manifested on transport i used to satisfy demands during transport j
$\boldsymbol{\mu}$	=	manifest vector
τ_{ij}	=	cargo manifested on transport i transferred to transport j

Presented as Paper 2010-8805 at the AIAA Space 2010 Conference and Exhibition, Anaheim, CA, 30 August–2 September 2010; received 3 August 2010; revision received 17 October 2010; accepted for publication 7 November 2010.

*Graduate Research Assistant, Department of Aeronautics and Astronautics, Room 33-409. Student Member AIAA.

†Research Scientist, Engineering Systems Division, Room E40-231. Member AIAA.

‡Associate Professor, Department of Aeronautics and Astronautics, Room 33-410. Associate Fellow AIAA.

I. Introduction

MANIFESTING resources and cargo onto launch vehicles and in-space transports is an integral part of planning space exploration. Past and present space missions reduced manifest complexity by limiting interdependencies between transports. The Apollo program used a sortie approach, in which all required cargo was carried on a single launch for each mission. In contrast, the International Space Station receives deliveries from many launches but only requires manifesting decisions across one transportation link; i.e., there is no intermediate transfer of cargo. These sortie and single-chain methods of manifesting will need to be expanded as humans seek to establish long-duration research stations and explore distant locations, including near-Earth objects, Lagrange points, and Mars. Future space exploration may depend upon on-orbit construction, refueling and depots, surface caching, and a host of other advanced logistics strategies. Furthermore, a well-planned manifesting strategy based on prepositioned, carry-along, and resupply cargo is essential for balancing risks, ensuring robustness against delays and cancellations, and achieving maximum exploration capability and success [1]. As a step toward this goal, this paper illustrates how a cargo manifest for extended exploration missions and campaigns can be obtained and optimized through relatively low computational effort such that the important feasibility constraints are met while maintaining tractability for integration into strategic analyses.

The manifesting problem is not limited to exploration in space. In 1804 Lewis and Clark set out on an extensive surface exploration reaching across the newly acquired American West from St. Louis to the Pacific Ocean. Before departure the expedition included extensive planning for trading with Native Americans, selection of wintering locations, and caching of goods to retrieve on the return voyage [2]. A century later, expeditions to the South Pole led by Scott, Shackleton, and Amundsen reinforced the importance of advance planning and depot establishment to survive the harsh Antarctic environment for months at a time [3]. Largely unaided by mathematical models, historical exploration relied on the expertise of

leaders coupled with a bit of luck for success and "living off the land." Modern terrestrial exploration embraces the use of airborne operations to significantly decrease travel time and provide resupply flexibility. "Food may also be sent in advance, but if distribution centers are within [helicopter] range it is more satisfactory to service the camp from these centers, thus providing fresh food and mail service," writes Blackadar [4] on arctic exploration in the 1950s.

Modern scientific approaches to logistics planning are prevalent in the military and business industry, broadly covered by the field of operations research. Rapid developments in computation have enabled the analysis of large-scale problems using mathematical models. Military logistics models focus on the routing and scheduling of vehicles and distribution of supplies from depots to combat units [5]. Baker et al. [6], for example, developed a large-scale linear programming model to optimize routing of people and cargo using several types of aircraft between multiple nodes. Within business applications, logistics models evaluate the frequency, capacity, route, and sequence of transports, as well as select depot and warehouse locations based on competition (quality, delivery time, etc.) and cost factors [7]. Klingman et al. [8], for example, developed a large-scale linear programming model to optimize the production and distribution of phosphate-based chemical products.

There are three major differences between space exploration systems and their modern terrestrial counterparts. First, space exploration operates on a long timescale. Exploring outside the Earth–moon system requires significantly longer durations (weeks and months), compared with terrestrial transport operations, which tend to unfold in hours and days, with the exception of ocean freight. The long-duration transports also contribute to in-flight demands, which may even exceed the demands at the destination. Second, space transportation schedules are highly constrained. Whereas on Earth scheduling transportation is generally flexible, space transports are limited by the astrodynamics of planetary motion and long lead time of spacecraft fabrication and ground operations. The schedule rigidity emphasizes the importance of advanced planning and robustness to uncertainty. Finally, space transportation cargo is extraordinarily critical. As there are no known resources in space or on planetary bodies to support life in raw form, and in situ processing capabilities rely on additional systems, even a slight undersupply corresponding to a resource or component could lead to serious failures. Furthermore, usable cargo comprises only 0.5–1.5% of a launch vehicle's wet mass to low Earth orbit, compared with nearly 50% of a truck's gross weight and 10% of an airplane's gross takeoff weight. These differences (timescale, schedule, and criticality) emphasize different aspects of the manifesting model for space exploration than that of terrestrial logistics operations.

Previous work established matrix-based methods for modeling the manifesting process, which was demonstrated with an analysis of the International Space Station resupply logistics and a lunar surface exploration campaign [9]. It was shown how the cargo manifests for a multiflight single-node scenario can be represented with a square **M** (manifest) matrix. An in-depth discussion was provided on the structure of the **M** matrix, its implications for campaign logistics, and its use for deriving various mission- and campaign-level logistics metrics.

The existing methods have been further expanded upon using a modeling framework developed for integrated space logistics simulation to allow for more general multitransport, multinode scenarios [10]. The expanded framework presented in this paper provides matrix-based methods for a wider range of scenarios under consideration for future exploration campaigns, including long-duration crewed missions, necessary for any exploration beyond low Earth orbit.

II. Matrix Modeling Framework

Matrices are a convenient notation for use in modeling frameworks, as they are compact and easily accessed within optimization functions. This section describes how both space exploration systems and cargo manifests can be represented in matrix form.

A. Modeling Space Exploration Systems

Previous work introduced matrix methods for modeling flight manifests using the assumption that there are several crewed and uncrewed flights carrying cargo to a specific location, or *node* [9]. Though past work used the concept of flights to deliver supplies, a more general modeling framework uses the notion of a *transport*, previously applied in the context of integrated space exploration logistics [10]. A transport is defined as the discrete movement of cargo up to a capacity limit from an origin node to a destination node with associated departure and arrival times. A transport may be a space flight (such as between the Earth and the moon), or a surface traversal (such as between two craters on the moon). The capacity limit represents the remaining capacity for cargo after considering any premanifested elements such as crew, science payloads, infrastructure, etc., and is typically expressed in either mass or volume units depending on the limiting constraint of the transportation system and analysis fidelity.

A *space exploration system* is a series of transports coupled with demands for cargo over time. Demands have both a temporal and spatial dimension, and cargo is assumed to be available for consumption during transport or immediately upon arrival and is shared by all colocated elements. In this simplified model, demands are limited to a single generic cargo class combining any underlying resources and packaging or overhead into one quantity to analyze the manifest in aggregate. Consumption of cargo means resources are used (removed from the scope of the model) to satisfy demands with no waste, empty packaging, or other byproducts generated. Though simplifying, these assumptions do not greatly affect the usefulness of the manifest model at a strategic level of analysis. First, in looking at a single transport capacity metric (e.g., mass or volume), all cargo is equivalent independent of function and finer-level detail is not necessary to create a manifest. Second, useless waste or byproducts generated during consumption would likely be discarded or jettisoned to avoid unnecessary use of cargo capacity. Finally, higher-level processes such as in situ resource utilization (ISRU) or environmental and life support system (ECLSS) processes, including water recovery, which depend on the transformation of resources (possibly byproducts of consumption) can be modeled outside the scope of the manifesting model using an integrated demand simulator. The resulting demand quantities therefore serve as an input to the manifesting model.

Demands for cargo occurring at nodes are aggregated by *exploration period*, defined as the interval between subsequent arrivals of transports or the end of the campaign. There exists exactly one exploration period for each transport, though each period need not include demands. Demand aggregation simplifies the model without loss of generality as no cargo could be delivered in the middle of an exploration period by definition. Similarly, demands for cargo that occur while in transit are aggregated to the start of the respective transport. Figure 1 illustrates a time-expanded network (bat chart) for a sample dual-launch lunar sortie. Kennedy Space

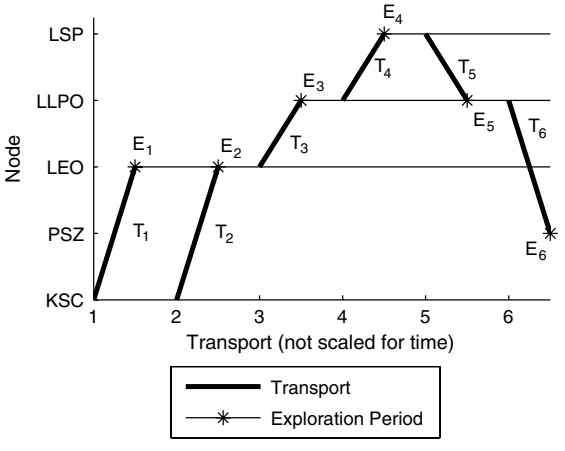

Fig. 1 Example bat chart showing transports and exploration periods.

Center (KSC) is the origin node from which two transports T_1 and T_2 emanate to deliver cargo to low Earth orbit (LEO). Two exploration periods E_1 and E_2 occur at LEO before transport T_3 departs for low lunar polar orbit (LLPO). Immediately upon arrival of T_3 exploration period E_3 occurs, followed by transport T_4 to the ultimate destination, the lunar south pole (LSP). The return to the Pacific splashdown zone (PSZ) uses transports T_5 and T_6 via LLPO.

Given this terminology, a space exploration system is completely defined in matrix format with seven components: the origin node vector $\mathbf{N_o}$, the destination node vector $\mathbf{N_d}$, the departure-time vector $\mathbf{T_d}$, the arrival-time vector $\mathbf{T_a}$, the transport capacity vector $\mathbf{C}$, the exploration demands vector $\mathbf{D_e}$, and the transport demands vector $\mathbf{D_t}$, as shown in Eqs. (1–7) for a campaign of n transports:

$$\mathbf{N_o} = [\, n_{o,1} \quad n_{o,2} \quad \cdots \quad n_{o,n} \,]^T \tag{1}$$

$$\mathbf{N_d} = [\, n_{d,1} \quad n_{d,2} \quad \cdots \quad n_{d,n} \,]^T \tag{2}$$

$$\mathbf{T_d} = [\, t_{d,1} \quad t_{d,2} \quad \cdots \quad t_{d,n} \,]^T \tag{3}$$

$$\mathbf{T_a} = [\, t_{a,1} \quad t_{a,2} \quad \cdots \quad t_{a,n} \,]^T \tag{4}$$

$$\mathbf{C} = [\, c_1 \quad c_2 \quad \cdots \quad c_n \,]^T \tag{5}$$

$$\mathbf{D_e} = [\, d_{e,1} \quad d_{e,2} \quad \cdots \quad d_{e,n} \,]^T \tag{6}$$

$$\mathbf{D_t} = [\, d_{t,1} \quad d_{t,2} \quad \cdots \quad d_{t,n} \,]^T \tag{7}$$

Table 1 defines the dual-launch lunar sortie exploration system in terms of these seven vectors.

The process of *manifesting* allocates cargo onto transports attempting to satisfy all demands without violating temporal or capacity constraints within the space exploration system, rendering it feasible from a logistics perspective. Propulsive feasibility is assumed to exist even if all flight capacities $\mathbf{C}$ are fully used.

B. Modeling Cargo Manifests

A space exploration system manifest is broken down into three components defining where and how cargo is used, illustrated in Fig. 2 for manifesting actions between transports i and j. Elements of the exploration utilization matrix $\mathbf{U_e}$, and transport utilization matrix $\mathbf{U_t}$, indicate cargo to be consumed to satisfy demands during exploration and transport, respectively. Elements from the transfer matrix $\mathbf{T}$ indicate cargo to be transferred from one transport to another for future utilization.

The element $u_{e,ij}$, as shown in Eq. (8) for a campaign of n transports, represents cargo brought by transport i that is consumed in exploration period j of the campaign:

$$\mathbf{U_e} = \begin{bmatrix} u_{e,11} & u_{e,12} & \cdots & u_{e,1n} \\ u_{e,21} & u_{e,22} & \cdots & u_{e,2n} \\ \vdots & \vdots & \ddots & \vdots \\ u_{e,n1} & u_{e,n2} & \cdots & u_{e,nn} \end{bmatrix} \tag{8}$$

Table 1 Dual-launch sortie exploration system definition

i	$n_{o,i}$	$t_{d,i}$, day	$n_{d,i}$	$t_{a,i}$, day	c_i, kg	$d_{t,i}$, kg	$d_{e,i}$, kg
1	KSC	0	LEO	1	100	25	25
2	KSC	2	LEO	3	500	0	25
3	LEO	4	LLPO	7	600	75	25
4	LLPO	8	LSP	9	300	25	250
5	LSP	14	LLPO	15	50	25	25
6	LLPO	16	PSZ	20	300	100	0

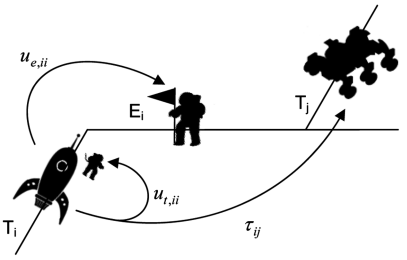

Fig. 2 Valid manifesting actions between transports *i* and *j*.

Cargo utilization between transports is only valid if both transports have the same destination node. Terms in the upper-triangular portion of the exploration utilization matrix represent prepositioned cargo (delivered before it was demanded), and terms along the diagonal represent carry-along cargo (delivered as it was demanded). If a demand cannot be satisfied during the exploration period in which it is needed, a future transport may satisfy the demand via a backorder (delivered after it was demanded). Backorders are represented in the lower-triangular portion of the exploration utilization matrix.

Crewed missions, especially ones with long-duration transports, are highly dependent on demands experienced during transit. These demands are different from exploration demands, because they must be satisfied by the transport in which they originate; i.e., prepositioning is not allowed. The element $u_{t,ij}$, as shown in Eq. (9) for a campaign of n transports, represents cargo brought by transport i that is consumed during transport j:

$$\mathbf{U_t} = \begin{bmatrix} u_{t,11} & u_{t,21} & \cdots & u_{t,1n} \\ u_{t,12} & u_{t,22} & \cdots & u_{t,2n} \\ \vdots & \vdots & \ddots & \vdots \\ u_{t,n1} & u_{t,n2} & \cdots & u_{t,nn} \end{bmatrix} \tag{9}$$

Transport utilization typically will only occur within a single transport, represented along the diagonal of the transport utilization matrix. If allowed, backorders are valid only if both transports have the same destination node and are represented in the upper- or lower-triangular portions of the matrix.

The element τ_{ij}, as shown in Eq. (10) for a campaign of n transports, represents cargo brought by transport i that is transferred to transport j:

$$\mathbf{T} = \begin{bmatrix} \tau_{11} & \tau_{12} & \cdots & \tau_{1n} \\ \tau_{21} & \tau_{22} & \cdots & \tau_{2n} \\ \vdots & \vdots & \ddots & \vdots \\ \tau_{n1} & \tau_{n2} & \cdots & \tau_{nn} \end{bmatrix} \tag{10}$$

Transfer of cargo does not necessarily indicate physical movement if the same underlying vehicles are used in both transports. A transfer is valid only if the destination node of transport i is the origin node of transport j and the arrival time of transport i is before the departure time of transport j. As a result of these constraints, transfer terms will only occur in the upper-triangular portion of the transfer matrix.

The resulting *manifest* $\boldsymbol{\mu}$ is the vector defined by the set of inputs that drive the movement of cargo throughout a campaign, given by the valid elements of the matrices $\mathbf{U_e}$, $\mathbf{U_t}$, and $\mathbf{T}$. The upper-bound manifest vector length is $3 \cdot n^2$, where n is the number of transports in the space exploration system. In practice, however, most of the elements are excluded from consideration, due to four spatial and temporal validity conditions restricting possible manifest actions, shown in Eq. (11):

$$\boldsymbol{\mu} \equiv \{\mathbf{U_e}, \mathbf{U_t}, \mathbf{T}\} \quad \forall \begin{cases} u_{e,ij} | n_{d,i} = n_{d,j} \\ u_{t,ij} | n_{d,i} = n_{d,j} \\ \tau_{ij} | n_{d,i} = n_{o,j} \\ \tau_{ij} | t_{a,i} \leq t_{d,j} \end{cases} \tag{11}$$

Furthermore, if backorders are not allowed, two additional conditions further restrict the supply of cargo for exploration and transport utilization. The transport utilization condition supersedes the previous constraint, resulting in five total constraints, as shown in Eq. (12):

$$\boldsymbol{\mu} \equiv \{\mathbf{U_e}, \mathbf{U_t}, \mathbf{T}\} \quad \forall \begin{cases} u_{e,ij} | n_{d,i} = n_{d,j} \\ u_{e,ij} | t_{a,i} \leq t_{a,j} \\ u_{t,ij} | i = j \\ \tau_{ij} | n_{d,i} = n_{o,j} \\ \tau_{ij} | t_{a,i} \leq t_{d,j} \end{cases} \tag{12}$$

The constraints require that exploration utilization is allowed for transports having identical destinations and arrivals before the demands are needed (constraints 1 and 2), transportation utilization is only allowed within a transport (constraint 3), and resource transfer is allowed for transports arriving and departing from identical nodes where the arrival occurs before the departure (constraints 4 and 5). Manifest vectors for a system with n transports and no backorders range from length $3 \cdot n$ for a purely sequential architecture to $(n^2 + 3 \cdot n)/2$ for a single destination architecture.

C. Exploration System Feasibility Criteria

A feasible space exploration system must satisfy three criteria: capacity constraints, demand satisfaction, and flow conservation. Capacity constraints ensure that the sum of exploration utilization, transport utilization, and transferred cargo does not exceed the capacity of each transport, as shown in Eq. (13):

$$\sum_j (u_{e,ij} + u_{t,ij} + \tau_{ij}) \leq c_i \quad \forall\ i \tag{13}$$

Demand satisfaction ensures that cargo is used to satisfy all exploration and transportation demands, as shown in Eqs. (14) and (15):

$$\sum_j u_{e,ji} = d_{e,i} \quad \forall\ i \tag{14}$$

$$\sum_j u_{t,ji} = d_{t,i} \quad \forall\ i \tag{15}$$

Flow conservation ensures that cargo is not created or destroyed outside of demand utilization within the exploration system (again, detailed ISRU and ECLSS operations are not modeled at the manifest level, these effects can be represented in the cargo demands). For each transport, the total cargo transferred in must equal the sum of cargo transferred out plus any exploration or transport demands used. To enable the instantiation of cargo at special source nodes (e.g., launch sites), any transports that originate from a set of nodes $\mathbf{S}$ are exempted. The resulting constraint is shown in Eq. (16):

$$\sum_j (\tau_{ji} - u_{e,ij} - u_{t,ij} - \tau_{ij}) = 0 \quad \forall\ i | n_{o,i} \notin \mathbf{S} \tag{16}$$

The space exploration system is considered feasible if a solution exists to a system of linear inequality equations based on the above constraints, summarized in Eq. (17):

$$\text{find } \boldsymbol{\mu} \text{ such that} \begin{cases} \mathbf{A_c} \cdot \boldsymbol{\mu} \leq \mathbf{C} \\ \mathbf{A_{de}} \cdot \boldsymbol{\mu} = \mathbf{D_e} \\ \mathbf{A_{dt}} \cdot \boldsymbol{\mu} = \mathbf{D_t} \\ \mathbf{A_f} \cdot \boldsymbol{\mu} = 0 \\ \boldsymbol{\mu} \geq 0 \end{cases} \tag{17}$$

The $\mathbf{A}$ matrices impose constraints on the manifest vector elements. $\mathbf{A_c}$ imposes capacity constraints from Eq. (13), $\mathbf{A_{de}}$ imposes exploration demand constraints from Eq. (14), $\mathbf{A_{dt}}$ imposes transport demand constraints from Eq. (15), and $\mathbf{A_f}$ imposes flow conservation constraints from Eq. (16). Finally, as the model only operates forward in time, manifest components cannot be negative.

By expressing the manifesting problem as a system of inequalities, linear programming (LP) methods can be used to find a solution and determine overall exploration feasibility. Under any objective function J, if the system of inequalities produces a solution, the exploration system is feasible. A simple but useful objective function is $J(\boldsymbol{\mu}) = \sum_i \mu_i$, which finds a minimum-flow manifest, avoiding needless circulation of cargo. In most feasible systems, a minimum-flow manifest is not unique and specific solutions may be obtained using other objective functions or additional constraints. In the event that a space exploration system is infeasible, the constraints may be relaxed; e.g., backorders may be allowed. If the modified exploration system is feasible, its Lagrange multipliers may be used to identify the most active constraints as suggestions for system modifications.

D. Flow-Network Graph Formulation

The manifesting problem, as described and formulated in Sec. II.C, essentially models the movement of cargo in a flow network. A time-expanded flow network enables analysis by reformulating the dynamic network as a series of static networks at each time step [11–13]. The extensive literature and tools of graph theory can then be applied to obtain insights into the exploration system problem, including new methods to establish feasibility and visual companions to matrices.

To model as a time-expanded flow-network graph, each transport is represented by a composition of four network-flow nodes: two designate the departure and arrival points of the transport and two notate the exploration and transportation demand sinks. Source transports replace the departure node with a source node. Arcs connect the nodes of one transport to others to represent valid cargo movement. In Fig. 3 we see the basic building block of a space exploration system represented as a glyph (a generic network component), with several flows entering and leaving the control volume: 1) used prepositioned cargo, 2) transfer cargo received, 3) dispatched transfer cargo, and 4) future prepositioned cargo.

The space exploration system can be formulated as a *minimum-cost flow problem* [11]. This type of flow network requires a unit cost and maximum capacity on each arc and a supply or demand associated with each node. In the space exploration system case, only the transportation arc between the departure and arrival node is bounded by the transport's capacity; all other arcs are unbounded. A minimum-flow manifest can be found if every arc is assigned the same nonzero unit cost. Also, all source nodes are connected to a virtual supersource node having supply equal to the sum of all transportation and exploration demands, and all sink nodes retain respective demands locally. The supersource node represents, in effect, the space enterprise supply chain (currently only available on Earth), which is the network of suppliers that creates the cargo items that are then subsequently transported and consumed during space exploration. In the long-term future such supersource nodes could potentially also exist on the moon, on Mars, and at other locations if the footprint of human civilization expand in this way.

Figure 4 illustrates the combination of transportation glyphs to construct a complete space exploration system flow-network graph corresponding to the dual-launch lunar sortie defined in Table 1. The supersource node supplying the two source (white) nodes representing the Kennedy Space Center is omitted for visual simplicity.

The minimum-cost flow problem is solvable in polynomial time for noninteger flows using numerous combinatorial algorithms [11].

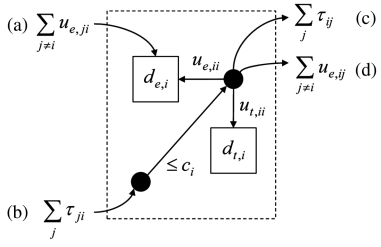

Fig. 3 Flow network glyph for transport *i*.

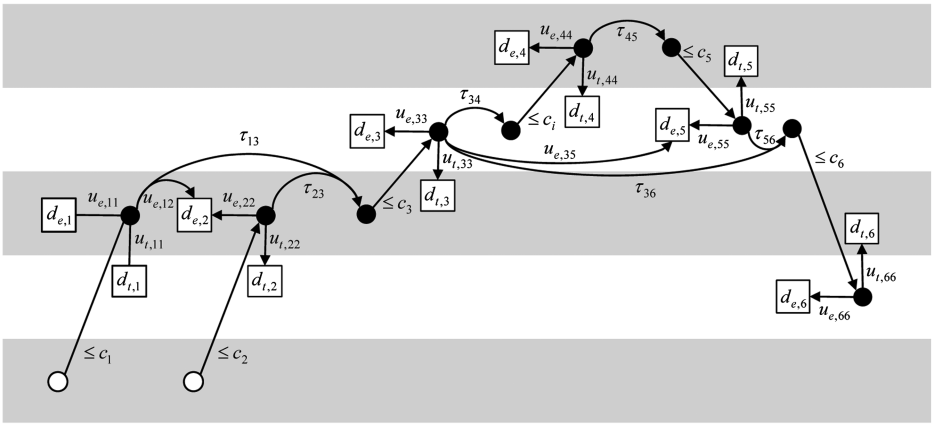

Fig. 4 Composite exploration system network-flow graph.

This is acceptable, given that the cargo considered in this analysis is quantized using mass or volume values and is therefore continuous. However, if cargo were to be discretized into logistics carriers such as cargo transfer bags represented with integer flows, the computational complexity of this problem would increase dramatically. Additionally, although system feasibility can be determined in polynomial time, finding the specific components of a network that contribute to the infeasibilities is computationally complex. However, polynomial time algorithms exist to identify a small set of nodes that together exhibit inherent infeasibility (called a *minimum witness*), which could be a subject of future research [14].

III. Manifest Optimization Methods

The transition from space exploration system feasibility to optimal manifesting methods involves only the selection of an objective function. This section describes the construction of relevant exploration system metrics and their application within manifest optimization.

A. Manifest Optimization

Once a space exploration system is deemed feasible, i.e., at least one valid manifest exists in which all conditions are satisfied, a specific solution may be tailored by using optimization objectives based on some desired logistics policy or strategy. A minimum-flow manifest, found using LP or flow-network methods, can be used as an initial manifest for optimization. The general form of the optimization is shown in Eq. (18), where $\boldsymbol{\mu}$ contains the valid manifest components and $\mathbf{A}$, $\mathbf{B}$, $\mathbf{A_{eq}}$, and $\mathbf{B_{eq}}$ enforce the feasibility constraints and any additional customized constraints for the specific space exploration system:

$$\min_{\boldsymbol{\mu}} J(\boldsymbol{\mu}) \text{ such that} \begin{cases} \mathbf{A} \cdot \boldsymbol{\mu} \leq \mathbf{B} \\ \mathbf{A_{eq}} \cdot \boldsymbol{\mu} = \mathbf{B_{eq}} \\ \boldsymbol{\mu} \geq 0 \end{cases} \tag{18}$$

Since the constraints take the form of a linear system of equations, if the objective function J is linear, then the optimization can use linear programming (LP) methods, though if J is nonlinear, then nonlinear programming methods are required. Potential objective functions may seek to minimize costs, distribute risk, improve robustness, or maximize prepositioned resources, or may consider some combination of these objectives. Nonlinear objective functions benefit from concepts and derived metrics from the **M** matrix and **D** matrix (described in the following section), which give a sense of cargo dependency between transports.

B. M Matrix and D Matrix Definitions

Previous work introduced the **M** matrix and **D** matrix as candidates for use in objective functions [9]. Element m_{ij} represents cargo manifested on flight i consumed during mission j and constitutes the square matrix $\mathbf{M} = [m_{ij}]_{n\times n}$ (for n flights in the campaign). Similarly, element δ_{ij} represents the dependency of flight j on flight i and forms the matrix $\mathbf{D} = [\delta_{ij}]_{n\times n}$. If there is only a single destination node with no transport demands, the **M** matrix is equivalent to $\mathbf{U_e}$. In other cases involving cargo transfer and transportation demands, several variations of the **M** matrix and **D** matrix can be devised from the manifest components.

1. *Utilization Manifest Matrix* $\mathbf{M_u}$

The closest notion to the original **M** matrix focuses on the total utilization of cargo, as shown in Eq. (19):

$$\mathbf{M_u} = \mathbf{U_e} + \mathbf{U_t} \tag{19}$$

In the utilization manifest matrix, element $m_{u,ij}$ captures the cargo manifested on transport i used during transport or exploration period j to satisfy a demand. The utilization manifest matrix, however, does not take into account the transfer of cargo between transports.

2. *Flow Manifest Matrix* $\mathbf{M_f}$

The utilization manifest matrix can be expanded to also include cargo transferred to other transports, as shown in Eq. (20),

$$\mathbf{M_f} = \mathbf{U_e} + \mathbf{U_t} + \mathbf{T} \tag{20}$$

though certain properties of the matrix (described in detail in [9]) no longer hold. For example, the sum of each column no longer corresponds to the demands for each period, due to cargo potentially being transferred multiple times over the course of a campaign. In the flow manifest matrix, element $m_{f,ij}$ captures the cargo manifested on transport i transferred to or used during transport or exploration period j to satisfy a demand.

3. *Source Manifest Matrix* $\mathbf{M_s}$

Each nonsource transport receives cargo from a supply chain of transports leading back in time to a source transport. The source manifest matrix captures the chain of transfers between a source transport and the point at which the cargo is used to satisfy a demand. Element $m_{s,ij}$ expresses the fraction of cargo that was originally manifested on transport i that contributed to utilization during transport or exploration period j to satisfy a demand.

To calculate the source manifest matrix, the utilization manifest matrix must first be combined with the transfer matrix to decompose the series of individual cargo movements. If a campaign contains n transports, at most $n-1$ decompositions are required to fold all cargo back to the origin node, which is the case for pure sequential transportation architectures. The first decomposition is simply the utilization manifest matrix. For each successive decomposition k, the contribution from transport i to j is the prior contribution from each nonsource transport l to j, weighted in proportion to the fraction of cargo transferred from transport i to l, as shown in Eq. (21):

$$m_{u,ij}^{k} = \begin{cases} m_{u,ij} & \text{if } k = 1 \\ \sum\limits_{l|n_{o,l}\notin S} m_{u,lj}^{k-1} \frac{\tau_{jl}}{\sum\limits_{h}\tau_{hl}} & \text{if } k > 1 \end{cases} \tag{21}$$

An important assumption in this formulation is that cargo is transferred to future transports in proportion to the contributions received from previous transports, meaning all transports supplying to a node where cargo may be mixed are partially involved in supplying cargo to future transports. Although this assumption does not explicitly hold in practice, the modeling approach presented does not attempt to assign manifest decisions for individual items and therefore does not distinguish cargo based on its origin.

Once the utilization decompositions have been evaluated, the source manifest matrix can be composed. Since the decomposition process does not include transports originating from a source node, the source manifest matrix sums contributions from all decompositions with a source transport contributing cargo utilization, as shown in Eq. (22):

$$m_{s,ij} = \begin{cases} \sum\limits_{k} m_{u,ij}^{k} & \text{if } n_{o,i} \in S \\ 0 & \text{otherwise} \end{cases} \tag{22}$$

4. Utilization Dependency Matrix $\mathbf{D}_u$

In the absence of backorders, the utilization dependency matrix captures the immediate nature of cargo utilization as carried-along or prepositioned. Element $\delta_{u,ij}$ represents the fraction of cargo from transport i that contributes to utilization during transport or exploration period j, as shown in Eq. (23):

$$\delta_{u,ij} = \frac{m_{u,ij}}{\sum\limits_{i} m_{u,ij}} \tag{23}$$

5. Source Dependency Matrix $\mathbf{D}_s$

Analogous to the utilization dependency matrix, the source dependency matrix captures the dependency of each transport on the source transports. Element $\delta_{s,ij}$ represents the fraction of cargo from source transport i that contributes to utilization during transport or exploration period j, as shown in Eq. (24):

$$\delta_{s,ij} = \frac{m_{s,ij}}{\sum\limits_{i} m_{s,ij}} \tag{24}$$

C. Transportation System Analysis

In addition to the **M** and **D** matrices, several other visualizations and derivative exploration system analysis metrics are described below. These metrics are useful for understanding space transportation networks and in the formulation of optimization objective functions.

1. Global Aggregate Feasibility

A necessary but not sufficient condition for exploration system feasibility can be expressed by global aggregate feasibility. To achieve feasibility from a global perspective, the cumulative capacity from all source transports must exceed the total cumulative demands (both transport and exploration) at all points in time. This can be expressed mathematically using Eq. (25), but is more useful when visualized as a plot over time:

$$\sum_{j\le i|n_{o,j}\in S} c_j \ge \sum_{j\le i} d_{e,j} + d_{t,j} \quad \forall\ i \tag{25}$$

The exploration system may be feasible if the cumulative source capacity line always exceeds the cumulative global demand line. Figure 5 illustrates the global aggregate feasibility of the dual-launch sortie defined in Table 1.

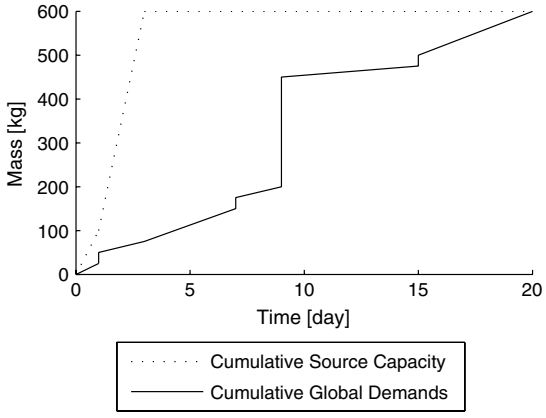

Fig. 5 Example global aggregate feasibility plot.

2. Exploration System Network

The exploration system network is a visualization showing the entire space exploration system definition in a time-expanded network similar to a bat chart. The transport lines are weighted in proportion to the demands occurring in transport and circles are weighted in proportion to exploration demands. The representation of nodes and arcs is similar to the network-flow formulation presented in Fig. 4, but simplified to omit demand sinks and manifesting arcs. Visual inspection can help identify bottlenecks in the transportation network that are not uncovered by global aggregated feasibility checks. Figure 6 illustrates a sample exploration system network based on the dual-launch sortie defined in Table 1.

3. Transport Criticality Index

The δ_{ij} components of the D matrices define the interdependence between transports, but they do not identify the impact of a transport on the overall exploration system. Transport criticality can be determined both for source dependency $\delta_{s,ij}$ and utilization dependency $\delta_{u,ij}$ components. Source dependency traces criticality back to the source transports (i.e., launches) while the utilization dependency identifies the criticality for a single link within the exploration system.

Transport criticality is composed of two components. The first component measures the extent of dependence on a transport based on cargo. It is calculated for transport i using Eq. (26):

$$\sum_{j} \delta_{\cdot,ij} \tag{26}$$

The second component measures the breadth of transports supplied. Transport j is supplied by i if it receives utilization or transfer cargo; i.e., $\delta_{\cdot,ij}$ is nonzero. It is calculated for transport i using Eq. (27):

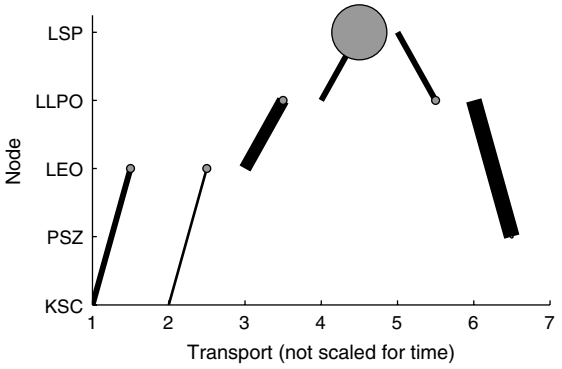

Fig. 6 Example exploration system network with weighted arcs and nodes.

$$\sum_j n_{\cdot,ij} \tag{27}$$

where

$$n_{\cdot,ij} = \begin{cases} 1 & \text{if } \delta_{\cdot,ij} > 0 \\ 0 & \text{if } \delta_{\cdot,ij} = 0 \end{cases}$$

A transport criticality (TC) plot is obtained by plotting the dependency breadth against the dependency extent. A line tracing the points $\sum_j \delta_{\cdot,ij} = \sum_j n_{\cdot,ij}$ serves as an upper bound for all transport criticalities. If a transport lies on this line on the TC plot, it means that it completely supplies all dependent transports; i.e., it is the sole carrier of the cargo that is subsequently needed by other transports that depend on it. The most crucial transports will be placed in the upper right of the plot, indicating a high extent of supply to a large number of transports. A sample TC plot for the dual-launch sortie is illustrated in Fig. 7 showing both source dependency and utilization dependency. In this example, transport 2 is the most critical source transport, and transport 3 is the most critical single transport link.

The composite transport criticality index (TCI) is defined as the Euclidean distance from the origin to a breadth-extent pair, shown in Eq. (28):

$$\text{TCI}_{\cdot,i} = \sqrt{\left(\sum_j \delta_{\cdot,ij}\right)^2 + \left(\sum_j n_{\cdot,ij}\right)^2} \tag{28}$$

This formulation places equal emphasis on breadth and extent as components of transport criticality.

4. *Capacity Utilization Index*

The capacity utilization index provides the ratio between cargo carried and a transport's total cargo capacity. It is calculated using the flow **M** matrix and the transport capacities, as shown in Eq. (29):

$$\text{CUI}_i = \frac{\sum_j m_{f,ij}}{c_i} \tag{29}$$

Though it may be desirable to maximize the capacity utilization index (CUI) across all transports, reaching the maximum value of 1 is nearly impossible for most exploration systems, because the demand constraint equalities and the flow conservation constraints do not allow a buildup of nonused cargo. In practice, any excess capacity after cargo manifesting could be used for additional payload (such as scientific equipment that is not explicitly modeled as demand) or contingency cargo. Once defined, these additional payload items would eliminate the excess capacity and result in a higher CUI.

5. *Logistics Strategy Index*

The logistics strategy index (LSI) is a ratio that indicates the amount of cargo prepositioned for future use versus the amount of cargo that is used during transport or in the exploration period that immediately follows. A value of 0 indicates all manifested cargo is used during the transport (or during its immediate exploration mission duration); i.e., it is a "carry-along" transport. A value of 1 indicates that all manifested cargo is used during future transports and associated explorations; in other words, it does pure pre-positioning. At the exploration level, the exploration LSI (eLSI) is calculated using Eq. (30):

$$\text{eLSI}_i = \frac{\sum_{j<i} m_{u,ji}}{\sum_j m_{u,ji}} \tag{30}$$

At the system level, the system LSI (sLSI) is calculated using Eq. (31), summing over all transports in the campaign:

$$\text{sLSI} = \frac{\sum_i \sum_{j<i} m_{u,ji}}{\sum_i \sum_j m_{u,ji}} \tag{31}$$

IV. Case Study: Lunar Surface Exploration

To demonstrate the optimization of cargo manifests in a relevant space exploration system, a sample lunar surface exploration system based on NASA human spaceflight program concepts is presented. The exploration system is defined and its feasibility is determined before optimizing cargo manifests under several objective functions. In this analysis, kilograms are used to set mass capacity limits for transports and demand quantities, though cubic meters (or similar units) could alternatively be used to capture volume constraints.

A. Case Study Summary

As of late 2009, the most current iteration of the lunar surface architecture released by NASA's Lunar Surface Systems Project Office (LSSPO) and the Constellation Architecture Team: Lunar (CxAT-Lunar) was scenario 12 [15,16]. In the described scenario architecture, successive missions (at a rate of about three per year) deliver infrastructure components to an outpost on the rim of Shackleton Crater at the lunar south pole. As infrastructure and supplies grow, explorations of increasing duration are enabled, leading up to continuous human presence. Because of the maturity of the campaign architecture, the exploration benefits from detailed element models based on prior analysis.

One of the interesting aspects of scenario 12 from a manifesting perspective is an emphasis on surface mobility elements for performing excursions to nearby locations, illustrated in Fig. 8. The lunar electric rover (LER) carries a crew up to 200 km on one charge. The all-terrain hex-limbed extraterrestrial explorer (ATHLETE) is capable of traversing difficult terrain while carrying a payload as large as a habitat or logistics module. In this case study the LER and the ATHLETE will be used to perform several surface excursions

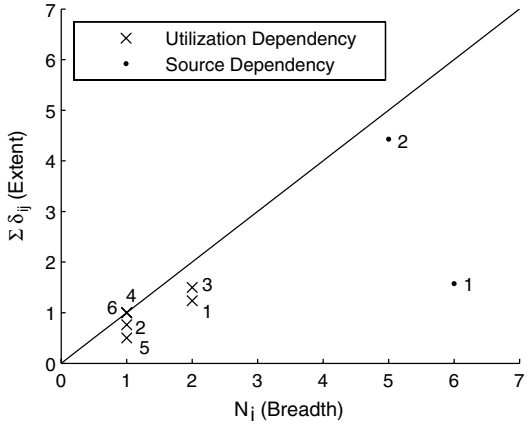

Fig. 7 Example TC plot.

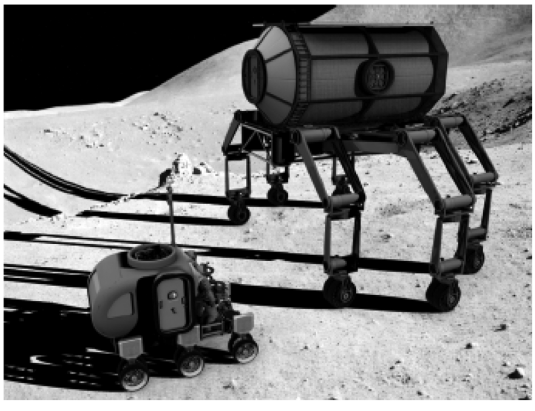

Fig. 8 Lunar surface mobility elements: LER (left) and ATHLETE (right), adapted from [15].

requiring additional manifesting to satisfy demands during transport and remote exploration.

B. Transportation System Definition

The exploration system is composed of 32 transports: 17 landings on the lunar surface (eight cargo and nine crewed with four astronauts each) and 15 surface transports supporting excursions, as illustrated in the bat chart in Fig. 9. A *mission* is notionally defined as the period of time between subsequent crewed or cargo landings inclusive of all surface transports. To simplify the exploration system definition, return transports for crewed missions are omitted as no demands are considered after ascent from the lunar surface. The complete exploration system definition is included in Table 2.

The first few missions establish basic infrastructure at the LSP. Mission 6 (transports 6–11) performs a surface excursion to the nearby Malapert Crater (MC) using LERs. A logistics LER traverses to a Malapert waypoint (MWP) to preposition contingency supplies a few days before the four crew members leave in two LERs. After reaching the waypoint, the crew continues two days to Malapert Crater and performs a seven-day local exploration. After exploration, the crew returns to the MWP waypoint, retrieves the logistics LER, and continues back to the base.

Missions 8 (transports 13–15) and 10 (transports 17–19) also include surface excursions to Malapert Crater, but without using the waypoint. Mission 8 performs a seven-day remote exploration while prepositioning a logistics carrier. Mission 10 performs a 14-day remote exploration before returning to the base with the logistics carrier.

Finally, mission 16 (transports 25–31) is largely composed of an extended 83-day surface excursion to the Schrödinger Basin (SB). A convoy of two crewed LERs and two ATHLETEs, one carrying a portable excursion module and one carrying a pressurized logistics module (PLM), passes two Schrödinger waypoints (SWP1, SWP2) on the way to the destination. The total transit to Schrödinger Basin spans 24 days, remote exploration spans 14 days, and the return transit spans 45 days.

To estimate demands for resources during surface transports and local exploration, including the effects of ISRU and ECLSS processes, the lunar exploration system was analyzed using SpaceNet, an open-source integrated modeling and simulation software tool [10]. An underlying discrete event simulator enables the instantiation of element models and definition of transports between nodes. Demands for resources are based on demand models both at the mission and element level. Mission-level demand models were used to establish required masses of scientific payloads. Element-level demand models were used to build up the remaining aggregated demand mass. Demands include crew consumables totaling 7.5 kg per person per day (after considering ECLSS processes) and spares for major infrastructure elements estimated at 10% of the element mass per year during active periods and 5% during inactive periods. SpaceNet demand integration also offsets crew demands for oxygen (2 kg/day) with any available ISRU plant oxygen, which is produced at a rate of 1000 kg per plant per year after plants are delivered in missions 6 and 12.

The lunar exploration system definition implies a buildup of a surface infrastructure at the LSP base. Supporting large amounts of infrastructure, along with longer crewed durations for later missions, creates a nonlinear composite demand model with significantly more demands toward the end of the modeling time frame. Figure 10 illustrates the increasing aggregated exploration and transportation demands throughout the scenario as more infrastructure to support is delivered. Detailed demand data are available in Table 2.

C. Transportation System Feasibility

The lunar exploration system meets the necessary feasibility condition from the global perspective, illustrated in Fig. 11. For many of the intermediate missions there is a margin between the maximum source capacity and global demands, though the margin decreases substantially after mission 14.

To verify system feasibility, Eq. (17) is used to formulate an LP problem. Under the validity conditions imposed by Eq. (12), $\boldsymbol{\mu}$ contains a total of 352 variables. Using the function `linprog`

Table 2 Lunar exploration system definition for lunar exploration campaign

Mission	i	$n_{o,i}$	$t_{d,i}$, day	$n_{d,i}$	$t_{a,i}$, day	c_i, kg	$d_{t,i}$, kg	$d_{e,i}$, kg	Comments
1.0	1	KSC	0	LSP	6	140	0	0	Uncrewed checkout exploration
2.0	2	KSC	184	LSP	190	310	0	339	Seven-day crewed sortie
3.0	3	KSC	549	LSP	555	4,210	0	13	Cargo delivery (incl. 2 LERs)
4.0	4	KSC	641	LSP	647	890	0	2,692	14-day crewed exploration
5.0	5	KSC	883	LSP	889	4,420	0	1,227	Cargo delivery (incl. 2 LERs)
6.0	6	KSC	944	LSP	950	825	0	727	28-day crewed exploration (total)
6.1	7	LSP	953	MWP	954	430	3	8	Logistics LER preposition at waypoint
6.2	8	LSP	957	MWP	958	690	54	22	Crewed LERs travel to Malapert waypoint
6.3	9	MWP	958	MC	961	690	161	215	Crewed LERs travel to Malapert Crater
6.4	10	MC	965	MWP	970	690	269	14	Crewed LERs travel to Malapert waypoint
6.5	11	MWP	970	LSP	971	1,120	57	1,922	Crewed and log. LERs return to base
7.0	12	KSC	1,249	LSP	1,255	8,460	0	727	Cargo delivery (incl. 2 tri-ATHLETEs)
8.0	13	KSC	1,280	LSP	1,286	930	0	3,059	28-day crewed exploration (total)
8.1	14	LSP	1,295	MC	1,298	1,640	169	394	Crewed and log. LER travel to Malapert
8.2	15	MC	1,305	LSP	1,308	2,040	169	2,549	Crewed and log. LER return to base
9.0	16	KSC	1,614	LSP	1,620	4,500	0	324	Cargo delivery (incl. 1 tri-ATHLETE)
10.0	17	KSC	1,645	LSP	1,651	1,100	0	1,489	50-day crewed exploration (total)
10.1	18	LSP	1,660	MC	1,663	950	170	792	Crewed and log. LER travel to Malapert
10.2	19	MC	1,677	LSP	1,680	720	170	4,200	Crewed and log. LER return to base
11.0	20	KSC	1,979	LSP	1,985	2,425	0	622	Cargo delivery (incl. 1 tri-ATHLETE)
12.0	21	KSC	2,040	LSP	2,046	1100	0	4,082	110-day crewed exploration
13.0	22	KSC	2,102	LSP	2,108	10,230	0	6,268	Cargo delivery
14.0	23	KSC	2,252	LSP	2,258	1,100	0	1,756	180-day crewed exploration
15.0	24	KSC	2,344	LSP	2,350	4,600	0	2,878	Cargo delivery
16.0	25	KSC	2,436	LSP	2,442	1,100	0	2,236	180-day crewed exploration (total)
16.1	26	LSP	2,463	SWP1	2,471	14,100	478	12	Crewed LERs and ATHLETEs travel to Schrödinger waypoint 1
16.2	27	SWP1	2,471	SWP1	2,479	14,750	477	7	Crewed LERs and ATHLETEs travel to Schrödinger waypoint 2
16.3	28	SWP2	2,479	SB	2,487	15,430	475	786	Crewed LERs and ATHLETEs travel to Schrödinger basin
16.4	29	SB	2,501	SWP1	2,516	15,430	897	3	Crewed LERs and ATHLETEs travel to Schrödinger waypoint 2
16.5	30	SWP2	2,516	SWP1	2,531	14,750	900	3	Crewed LERs and ATHLETEs travel to Schrödinger waypoint 1
16.6	31	SWP1	2,531	LSP	2,546	14,100	903	775	Crewed LERs and ATHLETEs return to base
17.0	32	KSC	2,557	LSP	2,563	10,500	0	6,895	Cargo delivery

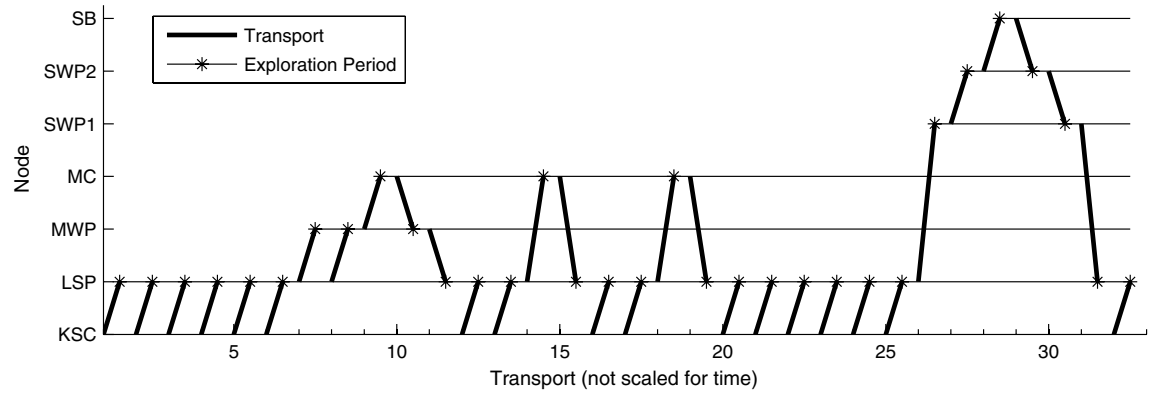

Fig. 9 Lunar exploration system bat chart.

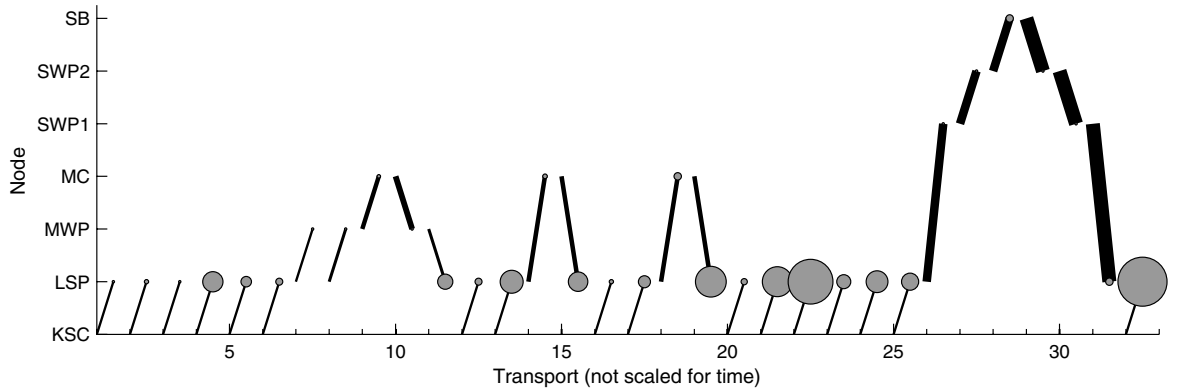

Fig. 10 Lunar exploration transportation network illustrating increasing demands.

within the MATLAB Optimization Toolbox™ and an objective function of $J(\boldsymbol{\mu}) = \sum_i \mu_i$ a minimum-flow manifest is found, establishing the lunar exploration system feasibility. The resulting TC plot for the minimum-flow manifest is illustrated in Fig. 12. It is interesting to note two groups of transports. One group is clustered in the top right (12, 3, 24, 22 and 5: all cargo transports) the other group is clustered in the bottom middle (such as 17, 13, 25, 4: mostly crewed transports). Transports in the top-right cluster are very critical since they are supplying a large fraction of cargo to a large number of other transports (up to 14 other transports). The bottom middle cluster supplies a much lower fraction of cargo to a fewer number of transports.

D. Dormant Cargo Limit Sensitivity Analysis

To expand upon the basic manifest model while reducing the problem scale, additional constraints limit cargo lifetime. As resources are treated as lumped mass, there is no available constraint for absolute lifetime (i.e., time between source transport and utilization), though a limit on dormant cargo time can be imposed as a proxy. Dormant cargo spans are defined as the time between cargo delivery and subsequent utilization or transfer to a later transport.

A variation of the validity constraints introduced in Eq. (12) is proposed to implement a dormant cargo limit $t_{\max}$. The modified set of validity constraints are summarized in Eq. (32):

$$\boldsymbol{\mu} \equiv \{\mathbf{U_e}, \mathbf{U_t}, \mathbf{T}\} \quad \forall \begin{cases} u_{e,ij} | n_{d,i} = n_{d,j} \\ u_{e,ij} | 0 \le t_{a,j} - t_{a,i} \le t_{\max} \\ u_{t,ij} | i = j \\ \tau_{ij} | n_{d,i} = n_{o,j} \\ \tau_{ij} | 0 \le t_{d,j} - t_{a,i} \le t_{\max} \end{cases} \tag{32}$$

This extra constraint creates an upper bound to prepositioning options and can significantly reduce the number of manifest variables as well as identifying limits of feasibility.

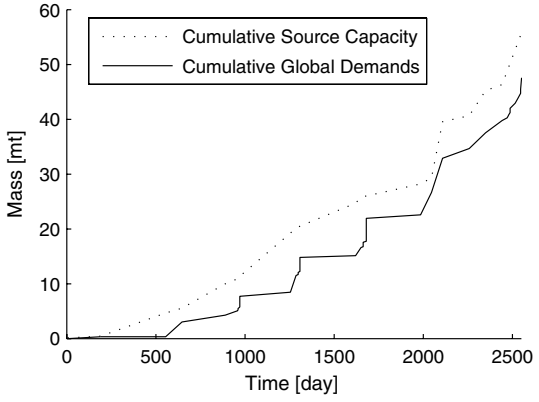

Fig. 11 Global aggregate feasibility plot.

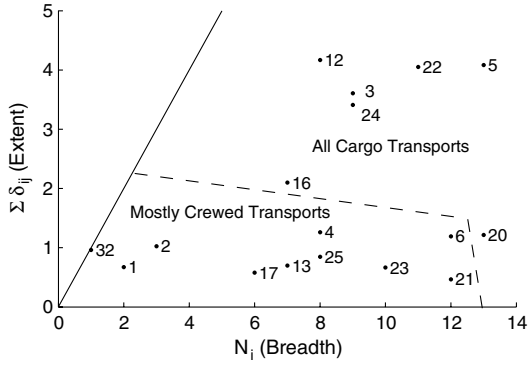

Fig. 12 Minimum-flow manifest source TC plot (sLSI = 0.5472).

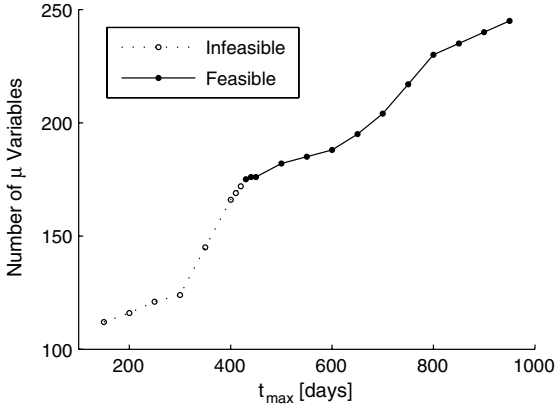

Fig. 13 Exploration feasibility sensitivity to cargo limitations.

A sensitivity analysis is performed to identify the exploration system feasibility dependence on dormant cargo limits. Both the number of remaining manifest variables and the resulting feasibility are summarized in Fig. 13. These results indicate that certain cargo must be capable of dormant periods of at least 430 days to achieve logistical feasibility for the lunar exploration system.

E. Cargo Manifest Optimization

Building off of the previous sensitivity analysis, a dormant cargo limit of 600 days is instituted for the cargo manifest optimization. The resulting manifest vector is reduced from 354 to 188 variables, substantially decreasing the nonlinear optimization computation time.

As a system-level measure of the underlying strategy for cargo manifests, the sLSI metric will form the basis of two optimization objective functions. The preposition strategy seeks to maximize sLSI, attempting to decouple each transport with its immediate exploration demands. The alternative carry-along strategy seeks to minimize sLSI, attempting to decouple exploration demands from as many transports as possible. While the first objective increases logistical robustness at exploration nodes by building up local safety stock, the second method decreases the likelihood that crew and cargo will be separated due to unforeseen events.

The optimization was performed using the `fmincon` function within the MATLAB Optimization Toolbox using a minimum-flow manifest as an initial solution and a functional tolerance of 10^{-9} as a convergence criterion for finding a local extrema. The optimized feasible sLSI for the preposition strategy was 0.6692 and for the carry-along strategy was 0.3320.

Comparative manifest analysis will use the metrics previously defined as the raw manifest matrices are unwieldy to process. The source TC plots, shown in Fig. 14, illustrate the general differences between the two strategies. Corresponding transports occupy similar regions between the two plots due to the nature of cargo versus crewed transports, but the preposition strategy stretches transports out over a larger breadth, indicating that the average transport is serving more exploration periods. This highlights a fundamental tradeoff between the carry-along and preposition strategies: pre-positioning increases transport criticality as defined.

The utilization transport criticality indices, shown in Fig. 15, emphasize the same point. Though only tracking one iteration of resource flow, most transports under the preposition strategy have a higher criticality. The mean TCI for the preposition transports is 3.02 with a standard deviation of 1.48, compared with a mean TCI of 1.99 and a standard deviation of 1.39 for the carry-along strategy.

The exploration-level logistics strategy indices (eLSI), shown in Fig. 16, highlight the selection of prepositioning for each transit using the system-level preposition strategy. Explorations 1, 7, 9, 26, 27, and 28 cannot take advantage of prepositioned cargo as these are the first transport to a new location (LSP, MWP, MC, SWP1, SWP2, and SB, respectively); therefore, their eLSI is zero by default.

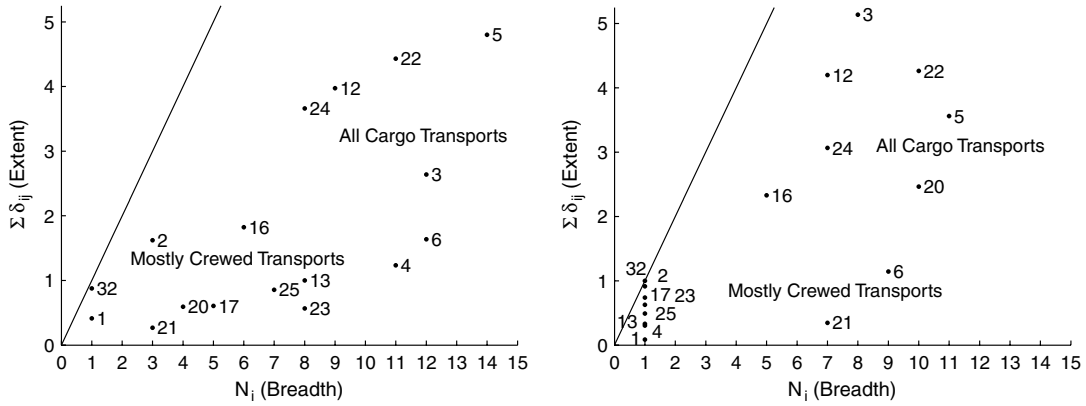

Fig. 14 Optimized manifest source TC plots: a) preposition strategy, sLSI = 0.6692 and b) carry-along strategy, sLSI = 0.3320.

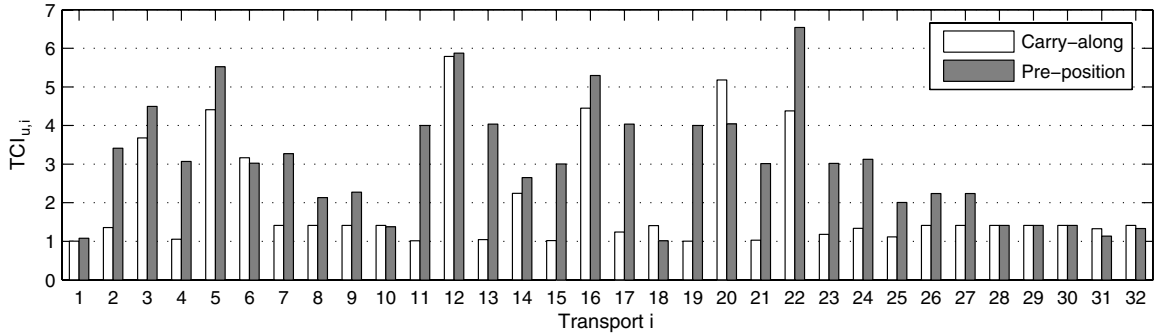

Fig. 15 Comparison of utilization transport criticality indices.

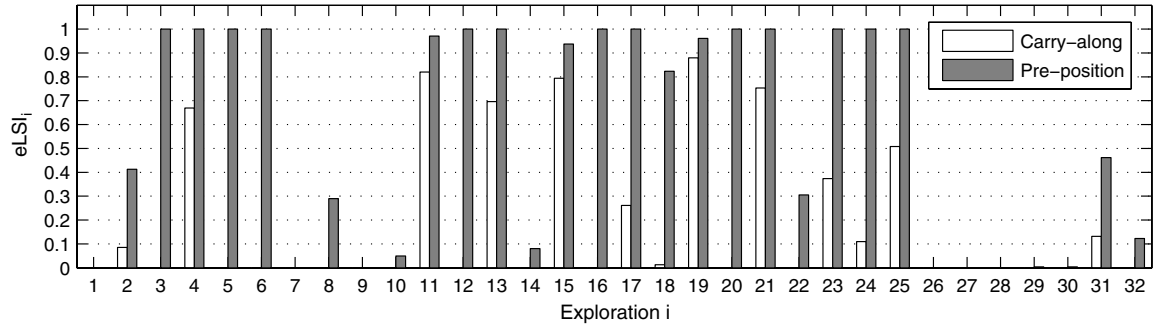

Fig. 16 Comparison of exploration logistics strategy indices.

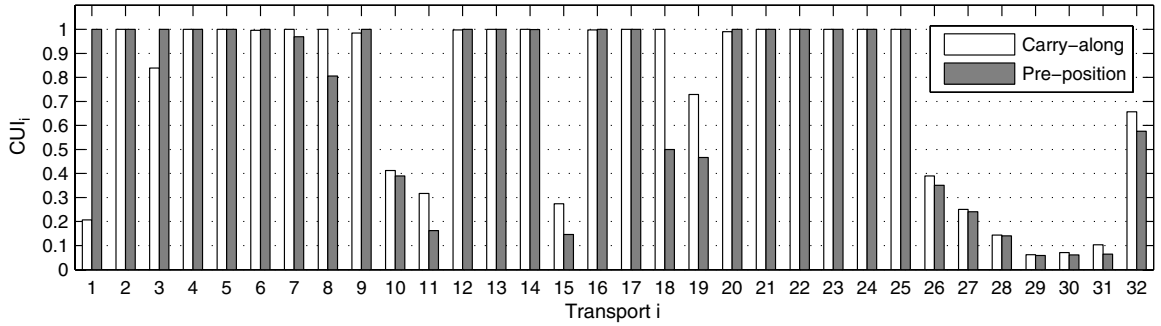

Fig. 17 Comparison of CUI.

The transport capacity utilization indices, shown in Fig. 17, are not much different between the two strategies except for the departing surface excursion transports (7, 8, 14, 18, and 25). Not constrained to find a minimum-flow manifest, the carry-along strategy transfers additional cargo over the entire excursion, some of which is used in place of prepositioned cargo opportunities. Which of the two manifesting strategies to use depends on the relative assessment of risk for emergence of undersupply situations at the LSP base (driven by reliability of in-space cargo transports) versus the likelihood of crew and cargo being separated during surface transports (reliability of crew transports).

V. Conclusions

This paper has shown how a matrix-based approach may be used to model and determine optimal manifests for multinode space exploration systems. Logistical feasibility can be determined using linear programming or flow-network graph methods to find a minimum-flow manifest. Finding an optimal manifest subject to a desired objective function requires the use of linear or nonlinear programming methods and a system objective function. Extensions of the basic modeling framework can also be used to determine feasibility sensitivity to other constraints such as dormant cargo limits. Strategies of maximizing prepositioned and carry-along cargo were presented as bookend cases, and additional objective functions balancing the two cases are a topic for further research.

For simplicity and tractability under optimization, the analysis has thus far treated all demands as an aggregated resource without differentiation between types of cargo. It may be possible to maintain tractability and distinguish cargo by functional class of supply, a concept implemented in other logistical models [17]. A natural extension of this manifest model would establish sources and sinks for each class of supply individually with capacity constraints enforced over all classes manifested on a transport. This extension may enable the explicit modeling of resource transformations to waste, recycling of waste back to useful resources, and the mining and utilization of in situ resources. A detailed manifesting model may also assign different priority levels for different resources. For example, crew provisions and spares needed for sustenance of crew and keeping vital equipment running would be of highest priority, followed by other types of supplies.

In addition to distinguishing between cargo class of supply, future modeling extensions may distinguish between cargo stowage environments. Many spacecraft have aggregate mass *and* volume capacity limits as well as constraints on masses of pressurized, unpressurized, gas, and liquid cargo that form a coupled system capacity. For example, a resupply vehicle may have capacity for 1500 kg of pressurized dry cargo and 1540 kg of liquid cargo, but only an aggregate capacity of 2350 kg across both environments. A coupled manifesting decision is required to determine the distribution between each cargo environment. Another extension of this work would allow for both Monte Carlo simulation of demand models as well as discrete event simulation of failed or delayed transports. The distribution of outcomes from such probabilistic models would allow selection of prepositioning versus carry-along manifesting strategies based on a quantitative assessment of various campaign uncertainties.

Finally, integration with the SpaceNet modeling environment is desired to improve integrated space exploration analysis. Many of the finer-level modeling details, including functional class of supply demand breakdowns and cargo environment differentiation currently exist or are under development within SpaceNet. Furthermore, the existing feasibility determination and cargo manifesting methods within SpaceNet are tedious and are in need of robust automation, similar to what could be provided with the presented methods. Future work is targeted at integrating the matrix-based optimal manifesting methods with the SpaceNet model.

References

[1] Shull, S., "Integrated Modeling and Simulation of Lunar Exploration Campaign Logistics," S.M. Thesis, Department of Aeronautics and Astronautics, Massachusetts Inst. of Technology, Cambridge, MA, 2007.

[2] Carr, D. L., *Into the Unknown: The Logistics Preparation of the Lewis and Clark Expedition*, Combat Studies Inst. Press, Leavenworth, KS, 2004; http://purl.access.gpo.gov/GPO/LPS59546 [retrieved 10 Oct. 2010].

[3] Pugh, L. G. C., "The Logistics of the Polar Journeys of Scott, Shackleton and Amundsen," *Proceedings of the Royal Society of Medicine*, Vol. 65, No. 1, 1972, pp. 42–47.

[4] Blackadar, R. G., "Field Methods and Logistics; Arctic Canada," *Geology of the Arctic*, University of Toronto Press, Toronto, 1961,

pp. 1095–1101.
[5] Kress, M., *Operational Logistics: The Art and Science of Sustaining Military Operations*, Kluwer Academic, Boston, 2002, pp. 17–36.
[6] Baker, S. F., Morton, D. P., Rosenthal, R. E., and Williams, L. M., "Optimizing Military Airlift," *Operations Research*, Vol. 50, No. 4, 2002, pp. 582–602. doi:10.1287/opre.50.4.582.2864
[7] Brandimarte, P., and Zotteri, G., *Introduction to Distribution Logistics*, Wiley, Hoboken, NJ, 2007.
[8] Klingman, D., Mote, J., and Phillips, N. V., "A Logistics Planning System at W. R. Grace," *Operations Research*, Vol. 36, No. 6, 1988, pp. 811–822. doi:10.1287/opre.36.6.811
[9] Siddiqi, A., de Weck, O., Lee, G., and Shull, S., "Matrix Modeling Methods for Spaceflight Campaign Logistics Analysis," *Journal of Spacecraft and Rockets*, Vol. 46, No. 5, 2009, pp. 1037–1048. doi:10.2514/1.43319
[10] Grogan, P., Armar, N., Siddiqi, A., de Weck, O., Lee, G., Jordan, E., and Shishko, R., "A Flexible Architecture and Object-oriented Model for Space Logistics Simulation," AIAA Space 2009 Conference and Exposition, AIAA Paper 2009-6548, Pasadena, CA, Sept. 14–17, 2009.
[11] Ahuja, R. K., Magnanti, T. L., and Orlin, J. B., *Network Flows*, Prentice–Hall, Upper Saddle River, NJ, 1993.
[12] Jarvis, J. J., and Ratliff, H. D., "Some Equivalent Objectives for Dynamic Network Flow Problems," *Management Science*, Vol. 28, No. 1, Jan. 1982, pp. 106–109. doi:10.1287/mnsc.28.1.106
[13] Silver, M., and de Weck, O., "Time-Expanded Decision Networks: A Framework for Designing Evolvable Complex Systems," *Systems Engineering*, Vol. 10, No. 2, 2007, pp. 167–186. doi:10.1002/sys.20069
[14] Aggarwal, C., Ahuja, J. H., Hao, J., and Orlin, J. B., "Diagnosing Infeasibilities in Network Flow Problems," *Mathematical Programming*, Vol. 81, 1998, pp. 263–280. doi:10.1007/BF01580084
[15] Mazanek, D. D., Troutman, P. A., Culbert, C. J., Leonard, M. J., and Spexarth, G., "Surface Buildup Scenarios and Outpost Architectures for Lunar Exploration," IEEE Aerospace Conference, IEEE Paper 2009-1093, Big Sky, MT, March 2009.
[16] Kennedy, K. J., Toups, L. D., and Rudisill, M., "Constellation Architecture Team—Lunar Scenario 12.0 Habitation Overview," NASA Johnson Space Center, Rept. JSC-CN-19362, March 2010.
[17] Shull, S., Gralla, E., de Weck, O., Siddiqi, A., and Shishko, R., "The Future of Asset Management for Human Space Exploration," AIAA Space 2006 Conference and Exposition, AIAA Paper 2006-7232, San Jose, CA, Sept. 2006.

P. Gage
Associate Editor